Human Molecular Genetics, 2011, Vol. 20, No. 12 **2322–2332**
doi:10.1093/hmg/ddr125
Advance Access published on April 12, 2011

Mutations in *PNKD* causing paroxysmal dyskinesia alters protein cleavage and stability

Yiguo Shen[1], Hsien-Yang Lee[1], Joel Rawson[1], Sunil Ojha[2], Patricia Babbitt[2], Ying-Hui Fu[1] and Louis J. Ptáček[1,3,*]

[1]Department of Neurology and [2]Department of Biopharmaceutical Sciences, University of California at San Francisco, San Francisco, CA 94158, USA and [3]Howard Hughes Medical Institute, San Francisco, CA 94158, USA

Received November 12, 2010; Revised January 31, 2011; Accepted March 23, 2011

Paroxysmal non-kinesigenic dyskinesia (PNKD) is a rare autosomal dominant movement disorder triggered by stress, fatigue or consumption of either alcohol or caffeine. Attacks last 1–4 h and consist of dramatic dystonia and choreoathetosis in the limbs, trunk and face. The disease is associated with single amino acid changes (A7V or A9V) in PNKD, a protein of unknown function. Here we studied the stability, cellular localization and enzymatic activity of the PNKD protein in cultured cells and transgenic animals. The N-terminus of the wild-type (WT) long PNKD isoform (PNKD-L) undergoes a cleavage event *in vitro*, resistance to which is conferred by disease-associated mutations. Mutant PNKD-L protein is degraded faster than the WT protein. These results suggest that the disease mutations underlying PNKD may disrupt protein processing *in vivo*, a hypothesis supported by our observation of decreased cortical Pnkd-L levels in mutant transgenic mice. Pnkd is homologous to a superfamily of enzymes with conserved β-lactamase domains. It shares highest homology with glyoxalase II but does not catalyze the same reaction. Lower glutathione levels were found in cortex lysates from *Pnkd* knockout mice versus WT littermates. Taken together, our results suggest an important role for the Pnkd protein in maintaining cellular redox status.

INTRODUCTION

Dystonia is the third most common movement disorder, affecting ∼30 of every 100 000 individuals worldwide. It is characterized by abnormal posture and involuntary muscle contraction (focal or generalized) (1–3). Paroxysmal non-kinesigenic dyskinesia (PNKD, DYT8) is an early-onset autosomal dominant movement disorder characterized by episodic attacks of any combination of dystonia, chorea and athetosis. Attacks can be precipitated by consumption of alcohol or coffee, hunger, fatigue, stress and menstruation (1,4,5). PNKD is a monogenic disease with nearly complete penetrance. We previously reported the discovery of Ala→Val substitutions in the PNKD protein at either seventh or ninth positions that cause the disease (4), and a third mutation (A33P) was recently reported in a separate study (6). The protein sequence of PNKD contains a β-lactamase domain, suggesting it belongs to an enzyme superfamily found from prokaryotes to primates. Human glyoxylase II, also named hydroxyacylglutathione hydrolase (HAGH), is the closest homolog of PNKD in *Homo sapiens* and catalyzes the second enzymatic step in the glutathione-dependent glyoxylase pathway which converts methylglyoxal (MG), a toxic by-product of glycolysis, to D-lactic acid (7). The shared β-lactamase domain of PNKD shows 44% identity and 58% similarity to HAGH.

The human *PNKD* gene contains 12 exons and encodes at least three different isoforms (4). The long (PNKD-L) and medium (PNKD-M) isoforms contain the β-lactamase domain in the C-terminus, and the short form (PNKD-S) contains three exons with no homology to any known protein. *PNKD* point mutations exist in the first exon and are shared by the long and short forms. Of the three isoforms, the long form is expressed only in the central nervous system (CNS), while the medium and short forms are widely expressed. Although the β-lactamase domains of PNKD-L and HAGH share a high degree of similarity, the normal function of

*To whom correspondence should be addressed at: Howard Hughes Medical Institute, Department of Neurology, University of California at San Francisco, 548F Rock Hall, MC-2922, 1550 4th Street, San Francisco, CA 94158, USA. Tel: +1 4155025614; Fax: +1 4155025641; Email: ljp@ucsf.edu

Pnkd-L and the molecular dysfunction of mutant PNKD-L remain unknown.

MG is an endogenous byproduct generated by several metabolic pathways, including glycolysis, lipid peroxidation and threonine catabolism, with glycolysis being the major source (7,8). MG, an active glycation reagent, is toxic and mutagenic due to the reactivity of its aldehyde group with guanine residues of DNA and amino acid nucleophiles. MG is generally found at very low levels in cells and is detoxified mainly through the glyoxalase pathway. MG reacts with reduced glutathione, forming a hemithioacetal that is converted to *S*-D-lactoyl-glutathione (SLG) by glyoxalase I. Glyoxalase II (HAGH in human) then hydrolyzes SLG to D-lactate and reduced glutathione (4,7). Glutathione is a prominent scavenger of reactive oxygen species in cells (9). Furthermore, in neurodegenerative diseases and animal models of brain injury, glutathione is a measure of neuronal redox status (10,11).

In this study, we focused on the long isoform of PNKD and characterized wild-type (WT) and mutant PNKD-L enzymatic activity, protein stability and cellular localization. We found the disease mutations decreased PNKD-L protein stability and prevent an N-terminus cleavage event. Pnkd-deficient mice have lower brain glutathione levels and impaired motor coordination. Our findings suggest that Pnkd-L is involved in regulating cellular redox status through a reaction regenerating reduced glutathione, and disease mutations cause more rapid degradation and decreased endogenous Pnkd-L levels in the cortex. We previously reported that PNKD-L localizes to cellular membrane in HEK293 cells, but a recent study suggested mitochondrial localization of PNKD-L in Cos7 cells (6). Here we sought to clarify whether these contradictory localization patterns were due to differences in the two cell lines used and to study localization in a more relevant ('neuron-like') cell line (SH-SY5Y) using our anti-PNKD antibodies.

RESULTS

Disease mutations affect PNKD stability

When expressing PNKD-L from cultured cells, we observed lower protein levels for the mutant versus WT protein. This result was confirmed for both long and short isoforms (Fig. 1A), suggesting that disease-causing mutations may affect protein degradation rates. We used cycloheximide (CHX) to halt protein synthesis and measured protein degradation rates of WT and MUT PNKD-L. The CHX-chase assay revealed shortened half-life of MUT PNKD-L in cultured cells (Fig. 1B). A ^{35}S labeled pulse chase assay further confirmed this difference in degradation rates (Fig. 1C). MUT PNKD-L is degraded faster than WT PNKD-L, resulting in lower protein levels. To further examine degradation *in vivo*, we crossed *mut-Tg* mice onto the knock-out (KO) background so that only mutant *Pnkd-L* was expressed in the brain, and compared the mutant protein with the WT protein in littermate controls (Fig. 1D). Pnkd-L protein levels decrease significantly when only the mutant *Pnkd-L* protein is expressed (lane 4), when compared with one copy of WT *Pnkd-L* in its littermates (lane 1). Transcript levels of *Mut-Tg Pnkd* are not significantly different from endogenous *Pnkd* (Supplementary Material, Fig. S1).

Proteins are degraded in different pathways, including proteasomes, lysosomes or by autophagy. We used specific inhibitors to determine which pathway(s) are responsible for degradation of WT and MUT PNKD-L. Proteasomal and lysosomal degradation pathways were blocked either independently or together and PNKD-L protein degradation was analyzed. In cultured HEK293 cells, overexpressed PNKD-L is found in both membrane and cytosolic fractions (Fig. 2A). PNKD-L accumulated in the membrane fraction with the inhibition of proteasome (lactacystine), lysosome (chloroquine) or both pathways (MG-132) (Fig. 2B, lanes 2–4). In addition, 3-MA, an inhibitor of autophagy, led to the accumulation of MUT (but not WT) PNKD-L compared with dimethyl sulfoxide (DMSO) control (Fig. 2B, lane 5), although to a lesser extent compared with proteasome inhibitors (Supplementary Material, Fig. S2). Integrin αV was used as a transmembrane protein control and is mainly degraded through the lysosomal pathway (Fig. 2B, lanes 3 and 4). Cytosolic PNKD-L WT and MUT proteins are primarily degraded through the ubiquitin–proteasome-dependent pathway (Fig. 2C, lane 2). This suggests that shortened half-life of the MUT protein results from autophagy of membrane-associated PNKD-L.

Cleavage of the WT PNKD N-terminus

When a FLAG tag is attached to the N-terminus of the PNKD-L WT, or PNKD-L MUT, or a homologous protein, HAGH, it can be detected on all but the PNKD-L WT form, even though both WT and MUT PNKD-L are expressed and detected by the anti-PNKD-L antibody (Fig. 3A). C-terminal Myc or FLAG tags can be detected in all fusion proteins (data not shown). We speculated that the N-terminal tag may be cleaved from WT proteins. To test this, we engineered clones to express the different isoforms as fusions with a larger tag (GFP) on the N-terminus (WT and MUT (both L and S forms), and a truncated N-terminus [amino acids 1–79 of PNKD (N79)]. Using an anti-GFP antibody, a cleaved band was detected in WT (both L and S forms) and N79 (its size slightly larger than GFP alone) indicating that some of the N-terminus was cleaved in both PNKD-L and S forms (Fig. 3B, Supplementary Material, Fig. S3A). The MUT forms do not show a cleavage product (Fig. 3B, lanes 4 and 6). Based on the size difference between cleaved GFP and GFP alone, the cleaved N-terminus was estimated to be ∼15–30 amino acids in length. We speculate that the cleavage resistance is caused by point mutations in N-terminus of PNKD-L, such as A7V, A9V (4) or A33P (6). To further test this hypothesis, we generated these disease-causing mutations (A7/9V, A33P) and additional point mutations at residues close to the human mutations (A15G, R16G). In addition, one-point mutation downstream of the cleavage site was generated (C85G). The A7/9V, A33P, A15G and R16G mutations are all cleavage resistant, while the C85G mutation has no effect on cleavage (Fig. 3C). In a CHX-chase assay, the A33P and A15G mutants also show faster degradation versus WT forms (Fig. 3D and Supplementary Material, Fig. S3B and C). These results demonstrate that point mutations within the

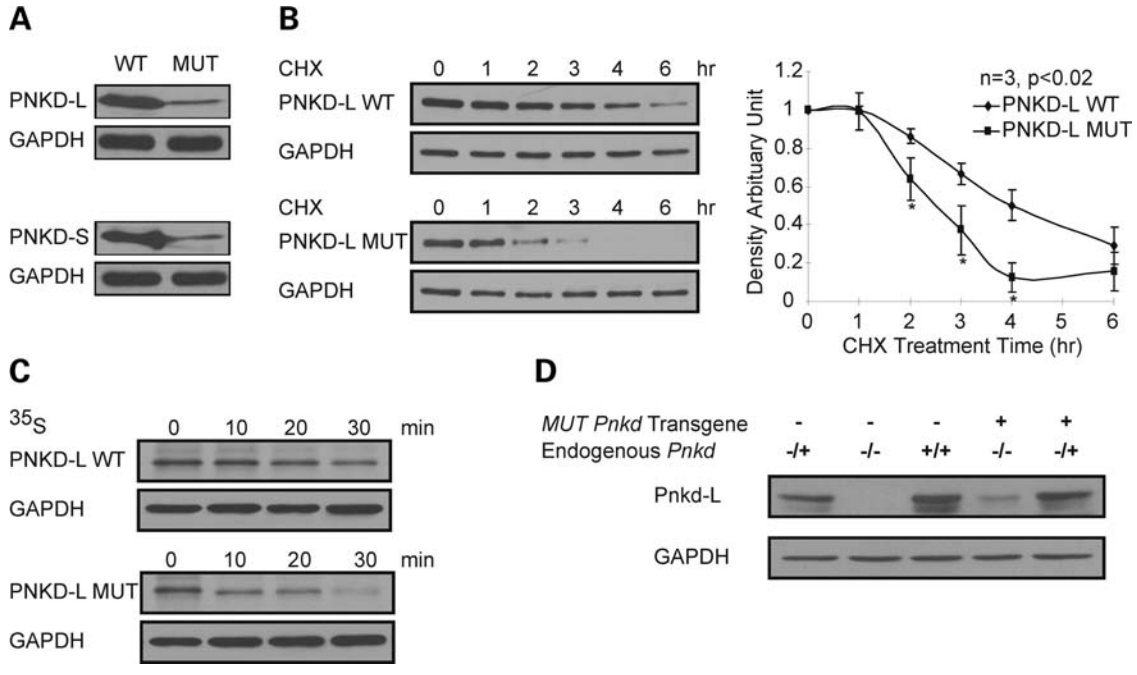

Figure 1. PNKD protein carrying disease mutations is degraded faster than WT PNKD. (**A**) HEK293 cells expressing MUT PNKD show lower protein levels than those expressing WT PNKD. PNKD-L WT and MUT (upper panel); and PNKD-S WT and MUT (lower panel) are shown. Equal volumes of soluble cell lysate were loaded in each lane. (**B**) The CHX assay in cells expressing WT or MUT PNKD long form. Cells were treated with CHX for 1, 2, 3, 4 or 6 h. Cells were transfected with 1 μg WT and 2 μg MUT to achieve similar protein levels at the 0 time point, data in the graph are from three independent experiments. Error bars indicate standard errors, $^{*}P < 0.05$ (Student *t*-test). (**C**) ^{35}S methionine-labeled Pulse Chase assay in cells expressing WT or MUT PNKD-L. Cells were collected at 0, 10, 20 or 30 min post-isotope labeling. (**D**) Pnkd-L protein levels in brain extracts from mice that carried different copy numbers of WT *Pnkd* and mutant *Pnkd* BAC transgene. The mutant BAC transgene in *mut-Tg* mice mimics endogenous *Pnkd* expression but has lower protein levels.

N-terminus of PNKD can prevent protein cleavage and are associated with decreased protein stability.

N-terminal mutations of PNKD-L do not affect WT protein stability

We next examined the ability of PNKD-L to multimerize. Fragments of PNKD-L were fused to the C-terminus of GFP, and co-transfected into cultured cells with Flag-tagged WT long form. PNKD-L multimerizes through an interaction of the N-terminal region and this interaction requires amino acids 132–166 (Fig. 4A). *PNKD* mutations do not interfere with this interaction (Fig. 4B). To test whether MUT PNKD-L might have an effect on the WT isoform, we tagged WT PNKD-L with GFP and co-expressed with FLAG-tagged PNKD-L WT or MUT in cultured cells and examined protein levels of the WT form (and *vice versa*) (Fig. 4C). Co-expression with WT or MUT PNKD-L did not significantly affect WT PNKD-L protein levels in cultured cells, suggesting that although PNKD-L can self-associate, the MUT PNKD protein does not destabilize WT PNKD *in vitro*. Similar studies with short and medium isoforms showed the same result. Although short and long isoforms can heteromultimerize, they do not affect WT protein levels (Supplementary Material, Fig. S4).

Subcellular localization of PNKD-L

A recent study suggested that PNKD-L localized to mitochondria in Cos7 cells (6) instead of cellular membrane (4) in HEK293 cells. To clarify this controversy, we repeated experiments with mitochondrial staining in Cos7 cells since our original experiments were in HEK293 cells. When overexpressed, both PNKD-L–FLAG and PNKD-L–GFP fusion proteins show strong cellular membrane-localization patterns in Cos7 cells, and no co-localization with mitochondria was found (Supplementary Material, Fig. S5). These findings were further supported by confocal microscopy of COS7 cells expressing PNKD–GFP (Supplementary Material, Fig. S6). Cellular fractionation of extracts of HEK293 cells overexpressing PNKD was also performed. Western blots showed no PNKD in fractions that were positive for a mitochondrial marker and abundant PNKD signal in the soluble fractions (Supplementary Material, Fig. S7). All PNKD isoforms and constructs were sequence confirmed.

We then performed experiments in a cell line that is more relevant to the expression pattern of PNKD. SH-SY5Y is a cell line derived from a human neuroblastoma. We transfected *PNKD-L* or *PNKD-L–GFP* fusion constructs into cultured SH-SY5Y cells and used two different approaches to examine the subcellular localization of PNKD-L: PNKD-L–GFP fluorescence, and immunostaining with an antibody against untagged PNKD-L. Representative cells expressing PNKD-L–GFP (Fig. 5A) and untagged PNKD-L stained with antibody (Fig. 5B) are shown, and the results suggest that PNKD-L is a membrane-associated protein.

In addition to membrane localization, we also observed some irregularly shaped cytoplasmic speckles in ~50% of the transfected cells, often close to the membrane. We then stained the cells with antibodies for the late endosomal

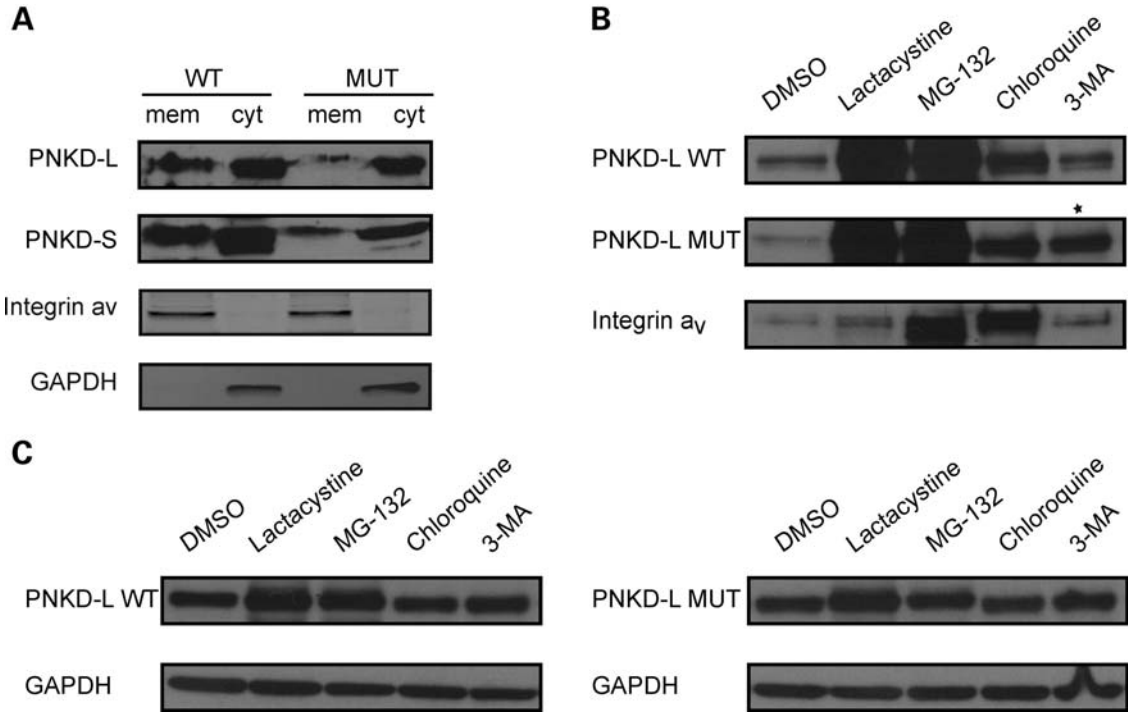

Figure 2. PNKD-L is degraded through the proteasomal, lysosomal and autophagy pathways. (**A**) The PNKD protein (upper panel PNKD-L and lower panel PNKD-S) is found in both membrane and cytosolic fractions. (**B** and **C**) Cells expressing equal amounts of WT or MUT PNKD-L were treated with DMSO, lactacystine (proteasome inhibitor), MG-132 (proteasome and lysosome inhibitor), chloroquine (lysosome inhibitor) and 3-MA (autophagy inhibitor), respectively, and lysates were extracted into membrane (B) and cytosolic (C) fractions. The membrane-associated WT PNKD-L protein is degraded through the proteasomal and lysosomal pathways (lanes 2–4), PNKD-L MUT is also degraded through the autophagy pathway (lane 5). The star marks the band with increased intensity of PNKD-L MUT proteins versus DMSO control when treated with 3-MA. (C) The cytosolic PNKD-L protein is degraded through the proteasomal pathway (lanes 2 and 3). Integrin αV and GAPDH were used as transmembrane protein and cytosolic protein controls, respectively.

marker M6PR and showed co-localization with PNKD-L, suggesting that cytoplasmic PNKD-L remains in late endosomes before trafficking to the cell membrane (Fig. 5C). No notable differences in localization of PNKD-L WT and MUT forms were seen in SH-SY5Y or HEK293 cells.

PNKD enzymatic activity assay

PNKD-L has a motif homologous to a conserved enzymatic domain. The C-terminal β-lactamase domain sequence similarity between human PNKD-L and HAGH is 58%, and leaves the unique 117 amino acid N-terminus of PNKD-L unaligned. HAGH hydrolyzes SLG to D-lactic acid and reduced glutathione. To test whether PNKD-L might hydrolyze SLG, we expressed and purified PNKD-L and HAGH from HEK293 cells using antibody cross-linked gel and measured SLG hydrolytic activity (Supplementary Material, Fig. S8). When incubated with SLG at 37°C, HAGH hydrolyzed SLG robustly. PNKD-L has extremely low but consistent SLG hydrolysis activity, showing an increasing hydrolysis within the range of soluble concentrations of SLG (0–1800 μM). This indicates that hydrolysis of SLG *in vivo* by PNKD-L is unlikely to be physiologically relevant. To further examine whether PNKD-L can efficiently hydrolyze SLG *in vivo*, we tested the ability of human PNKD-L to rescue HAGH activity in a *Drosophila melanogaster* strain lacking endogenous HAGH activity due to the presence of a homozygous null mutation in the *Drosophila hagh* gene (CG4365, Fig. 6A). Introduction of a *Drosophila* HAGH transgene into the null background restores HAGH activity to a higher level than that observed in the WT fly, while introduction of a human *PNKD-L* transgene into the same null background shows no rescue of SLG metabolism, further supporting the idea that PNKD-L does not use SLG as an *in vivo* substrate.

Sequence alignment and enzyme kinetics suggest that PNKD-L substrate may be an (as yet, unknown) α-hydroxythioester, and similar to HAGH, PNKD-L may be involved in a chain reaction to detoxify an α-ketonaldehyde product in CNS neurons using reduced glutathione (GSH) as a co-factor. The mutant *Pnkd* transgene or knockout of *Pnkd* may cause accumulation of some α-hydroxythioester and reciprocally decrease neuronal GSH. To test this hypothesis, we measured GSH levels in the frontal cortex in a cohort of 15-week-old *Pnkd* null mice (*KO*, $n = 8$), *mut-Tg* mice (*mut-Tg*, $n = 12$) and WT ($n = 13$) littermates. Figure 6B shows that *KO* and *mut-Tg* mice have significantly lower glutathione levels (~20% lower) in the frontal cortex compared with WT littermates, suggesting that glutathione-related metabolic changes are present in these mice even when there is no attempt to precipitate attacks.

DISCUSSION

PNKD is a movement disorder with symptoms precipitated by stress and alcohol or caffeine consumption. PNKD patients appear completely normal between attacks (1,4,5), although

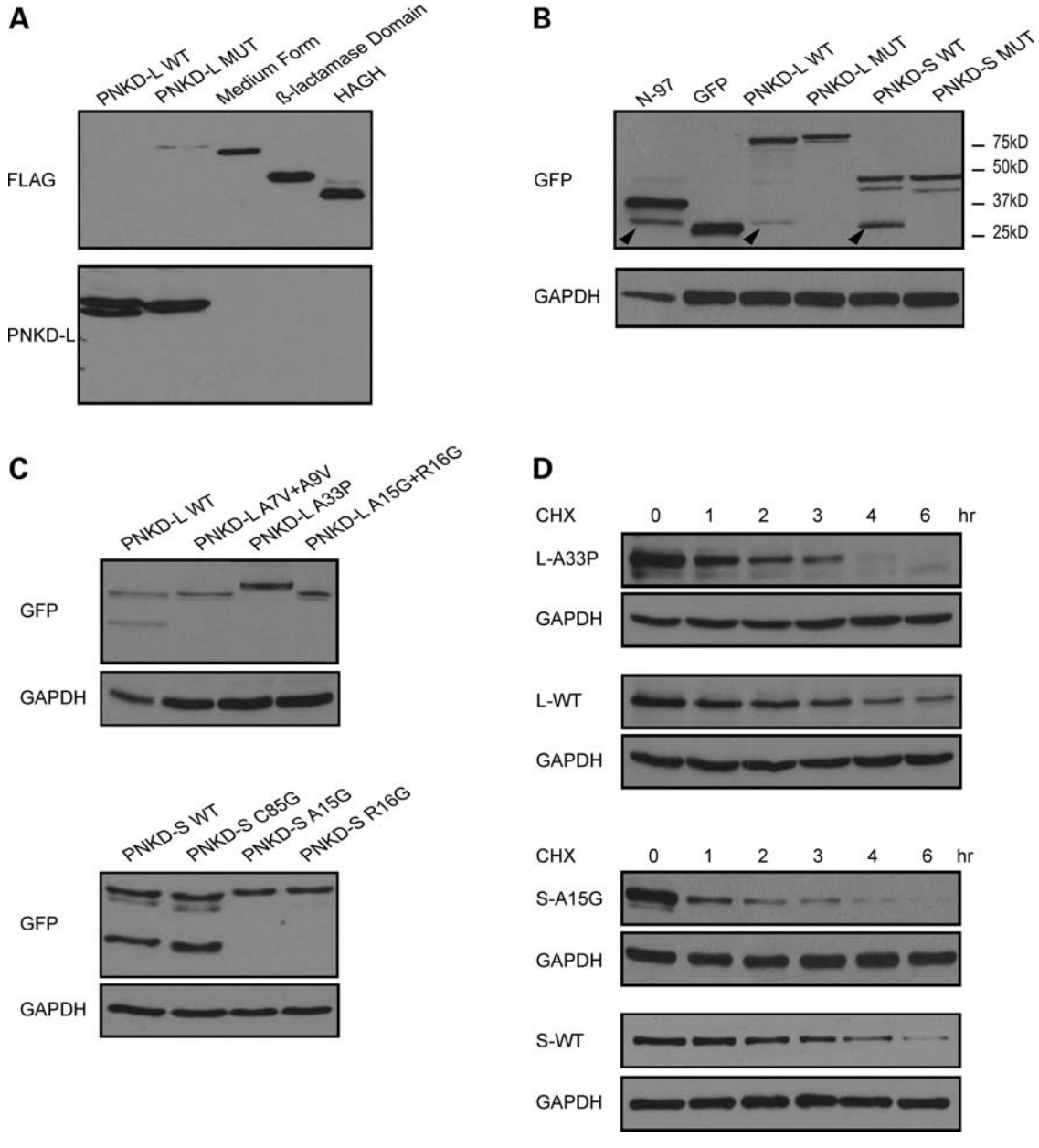

Figure 3. WT PNKD-L is cleaved at its N-terminus, while mutant PNKD-L is resistant to cleavage. (**A**) A FLAG epitope was added to the N-terminus of PNKD-L WT or MUT, PNKD-M, PNKD β-lactamase domain, and HAGH. Cell lysates were blotted with FLAG or PNKD-L antibody. (**B**) GFP was fused to the N-terminus of PNKD-L WT or MUT, PNKD-S WT or MUT, and a fragment containing amino acids 1–79 of the PNKD N-terminus (N-79). Cell lysates were blotted with GFP antibody. Cleaved GFP was detected in all constructs that contain WT N-terminal sequences, the arrowheads indicate the cleaved N-terminal GFP fragments which are slightly larger than GFP alone. (**C**) GFP was fused to the N-terminus of PNKD-L WT, MUT, A33P, A15G/R16G or PNKD-S WT, C85G, A15G and R16G. GFP cleavage was only detected in WT and C85G. (**D**) The CHX assay in cells expressing PNKD-L A33P and WT, PNKD-S A15G and WT shows that these mutations also lead to faster degradation.

there is anecdotal evidence of increased migraine prevalence in PNKD patients (L.J.P., unpublished data). The C-terminus of Pnkd-L is homologous to human HAGH, which is important for the second catalyzed step in MG detoxification. MG is a toxic byproduct of glycolysis and exists in many natural products including alcohol and coffee (12). We show that PNKD-L recognizes the same substrate in this pathway (SLG), but catalyzes the same reaction as HAGH at a very low level, suggesting that a similar α-hydroxythioester substrate is likely to be the physiologically relevant substrate for PNKD-L activity in the CNS (13,14). PNKD-L may function in a pathway(s) to detoxify an α-ketonaldehyde product in cells using GSH as a co-factor in CNS neurons, as suggested by decreased GSH levels in *Pnkd KO* mice. The *in vivo* substrate(s) for PNKD-L is unknown but GSH levels in cortical lysates from *Pnkd KO* mice were decreased, suggesting the reaction catalyzed by Pnkd-L may be important for regeneration of GSH in CNS neurons. GSH is essential for

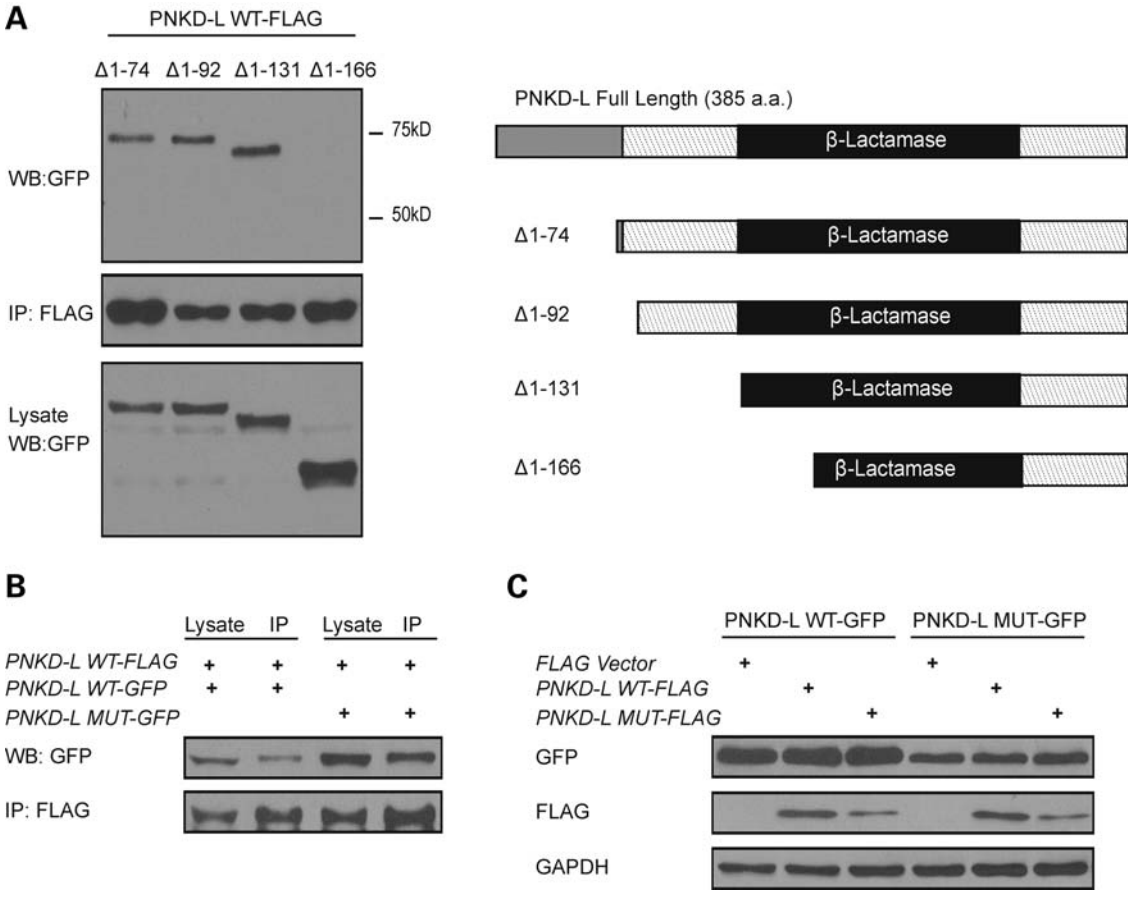

Figure 4. PNKD can self-associate, but PNKD-MUT does not have a dominant negative effect on WT protein levels. (**A**) *PNKD-L WT* subclones of different lengths were ligated into GFP vectors (C-terminal) and tested for possible association with FLAG-tagged (C-terminal) PNKD-L WT by Co-IP. The shaded rectangle indicates the 1–79 amino acids. N-terminal sequence shared by long and short isoforms, dark rectangle indicates the β-lactamase domain. The C-terminal 219 amino acid fragment of PNKD-L does not associate with PNKD-L. (**B** and **C**) FLAG-tagged (C-terminal) *PNKD-L WT* and *MUT* were co-transfected into HEK293 cells with GFP-tagged (C-terminal) *PNKD-L WT* and *MUT*. Cells were transfected with the same amount of DNA. (B) The protein was precipitated by an anti-FLAG M2 agarose (Sigma) and the elution was blotted for associated protein using a GFP antibody. (C) Protein levels of WT or MUT forms were detected by an anti-FLAG or anti-GFP antibody. No change in protein levels was found when co-expressing WT and MUT isoforms.

maintaining proper cellular redox status and protecting against toxicity and other stress conditions that may occur in neurons (11,15). Neurons are vulnerable to stress conditions such as hypoxia, ischemia, altered pH and oxidative stress. Such conditions are often accompanied by an increased presence of cellular reactive oxygen species and decreased levels of cellular GSH (16). Reactive oxygen species are free radicals or reactive molecules containing oxygen atoms, such as superoxide or hydrogen peroxide, and are cleared from cells by the action of superoxide dismutase or glutathione peroxidase. GSH is an important factor involved in clearing reactive oxygen species, and the level of GSH is an indicator of cellular redox status (17,18). It has been reported that increased levels of GSH can protect against neuronal death caused by kainic acid or glutamate toxicity (10,19,20). Conversely, reduced GSH levels contribute to neuronal death in Down's syndrome and ALS-like transgenic mouse models (17,21). In our Pnkd-deficient mice, GSH levels were ∼20% lower in the cortex, suggesting impaired redox regulation.

In the present study, we characterized an N-terminal cleavage event and measured protein stability of PNKD-L. The mutant PNKD-L isoform is resistant to N-terminal cleavage and is less stable than the WT protein. Levels of the mutant PNKD-L protein in *mut-Tg* X *Pnkd*$^{-/-}$ mouse brains (with one to two copies of mutant *Pnkd* transgene) are lower than endogenous WT Pnkd-L in WT heterozygous littermate brains.

PNKD-L is specifically expressed in the CNS; the membrane and endosome localization pattern suggests that PNKD-L may be involved in vesicle recycling or membrane protein transport in CNS neurons. When neurons are under stress or undergoing dramatic changes in redox status, mutant PNKD-L may fail to maintain necessary levels and lead to malfunction of motor circuits. Another possibility is that post-translational modification may affect PNKD-L itself or the associated protein complex *in vivo* function in CNS neurons. It has been reported that disease mutations in the TorsinA protein affect the protein stability, nuclear envelope, cellular trafficking of the dopamine transporter to the cellular membrane and also have an effect on synaptic vesicle recycling in SH-SY5Y cells (22–28). There is a growing body of evidence suggesting that dopaminergic neurons are

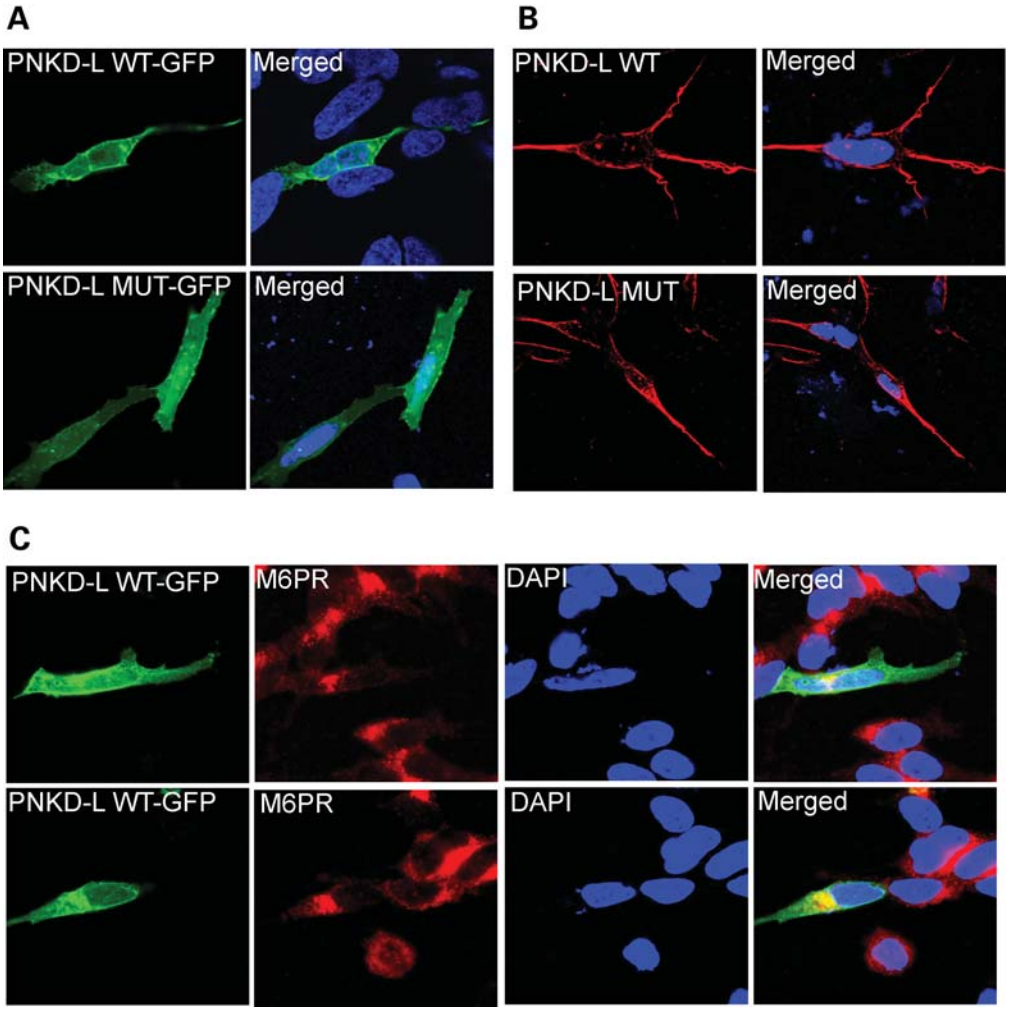

Figure 5. Cellular localization of the long PNKD isoform. *PNKD* constructs were transfected into SH-SY5Y cells to express PNKD-L or PNKD-L–GFP fusion protein (C-terminal tag). (**A**) PNKD-L–GFP WT and mutant (MUT) forms are localized to the cellular membrane; (**B**) immunostaining of PNKD-L WT and MUT forms with PNKD-L antibody; (**C**) PNKD-L–GFP is localized to both the cellular membrane and late endosomes, indicated by mannose 6 phosphate receptor (M6PR) immunostaining. Cellular localization patterns of PNKD-L in (A) and (C) are in an approximate 1:1 ratio in transfected SH-SY5Y cells.

affected in mouse models of generalized dystonia and PNKD (26,29, *Lee et al.*, submitted for publication). Identifying PNKD-L-associated proteins involved in membrane protein trafficking in CNS dopaminergic neurons will likely address this issue and increase our knowledge of the molecular mechanism of dystonia.

We have previously shown that the long isoform of PNKD is localized to the cellular membrane in HEK293 cells, the medium isoform to mitochondria and the short isoform is widely distributed in cells (4). A recent study showed a contradictory localization pattern in Cos7 cells where PNKD-L and PNKD-S isoforms localized to mitochondria and PNKD-M localized to the Golgi apparatus, ER and plasma membrane (6). We reasoned that these disparate results may have been explained by the use of different cell lines. However, when we repeated these experiments in Cos7 cells, we still observed a membrane-localization pattern with some cytosolic pellets for both human PNKD-L–GFP and PNKD-L–FLAG constructs that did not co-localize with mitochondrial markers (Supplementary Material, Figs S5–S7) (4). Since *PNKD-L* is specifically expressed in CNS neurons, we chose a neuroblastoma-derived cell line SH-SY5Y (as a 'neuron-like' cell line) and have shown that PNKD-L is specifically localized to the cell membrane and late endosomes. SH-SY5Y is a cell line derived from a human neuroblastoma cell line, and HEK293 cells were derived from human kidney epithelia. PNKD-L antibody staining revealed that the long isoform of human PNKD localizes in a cell membrane pattern in both cell lines. Similar findings were seen when cells were transfected with a clone encoding a PNKD-L–GFP fusion protein. A localization pattern of endogenous Pnkd-L in cultured primary neurons or brain slices would address this issue. However, due to the low protein levels of endogenous Pnkd-L, immunostaining in mouse brain slices and cultured primary neurons failed to generate high-resolution images of cellular localization. We considered the possibility that a sequence variant or mutation in the constructs used in these studies might be causing our disparate results, but we resequenced all constructs used and they were confirmed to be correct. Another possibility worth investigating involves the antibodies used by Ghezzi *et al*. All of the

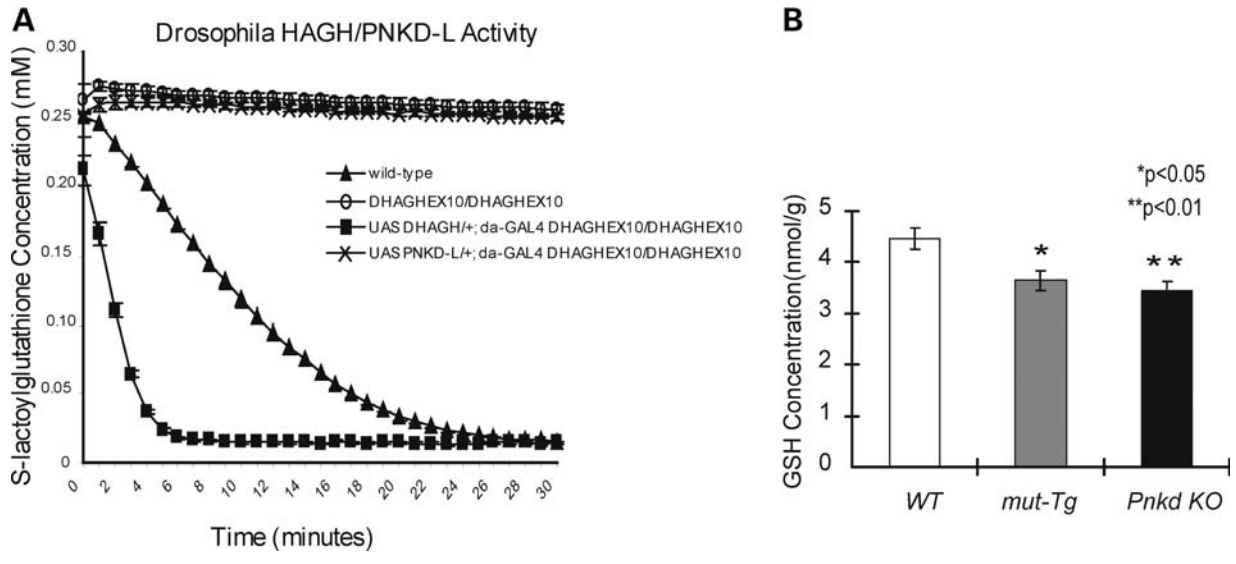

Figure 6. PNKD-L does not rescue lost HAGH activity. (**A**) Protein extracts from a *Drosophila* HAGH homozygous null mutant (circles) lose the ability to hydrolyze SLG when compared with protein extracts from WT flies (triangles). When *Drosophila* HAGH is replaced in the null mutant background by transgenic over-expression (squares), SLG hydrolytic activity is restored to levels even greater than detected in WT flies (triangles). However, when human PNKD-L is expressed on a *Drosophila* HAGH mutant background, no rescue of SLG hydrolysis is detected (x's). (**B**) *Mut-Tg* mice and *KO* mice have lower glutathione levels in extracts from the cortex compared with WT littermates under normal conditions. Error bars indicate standard errors (WT, $n = 13$; mut-Tg, $n = 12$; *KO*, $n = 8$). $^{*}P < 0.05$ and $^{**}P < 0.01$ from WT mice (Student's *t*-test).

antibodies used for the immunofluorescence co-localization studies were generated in mice (Figs 3 and 5 and Supplementary Material, Fig. S1 in ref. 6), it is possible that there was cross-staining by secondary antibodies. There was insufficient detail in the description of methods regarding the antibodies used and of primary antibody incubation sequence to assess this possibility. We chose antibodies from different species (mouse and rabbit) to avoid cross-staining, and we also used GFP fusion proteins and MitoTracker dye for co-localization studies (Fig. 5 and Supplementary Material, Figs S5 and S6). We consistently observed a cellular membrane-localization pattern for PNKD long form. Another possible explanation is that *PNKD* was expressed at much higher levels in the studies of Ghezzi *et al*. and that this led to aberrant expression of the protein. Again, insufficient details are given to allow assessment of this possibility.

In addition to microscopy, we also looked into the mitochondrial protein database for all PNKD isoforms. MitoCarta is an inventory of >1000 mouse genes encoding proteins with strong support for mitochondrial localization (30). This database was generated by performing mass spectrometry of mitochondria isolated from 14 tissues, assessing protein localization of GFP-tagged fusion proteins, and using a Bayesian approach to integrate these results with six other genome-scale data sets of mitochondrial localization. In querying the mass spectrometry data set for peptides from the PNKD protein, there was strong support for the short isoform to be localized to mitochondria with two peptides unique to this isoform being seen multiple times in multiple tissues (Supplementary Material, Fig. S9). In contrast, no peptides were seen from the β-lactamase domain of PNKD-L and PNKD-M. One peptide shared between the long and short isoforms was seen only rarely and not in any of the four CNS tissues. Absence of peptides in the database does not absolutely prove that a protein is not localized in mitochondria. However, in light of other data presented here, it further supports our claim that PNKD-L is not mitochondrial.

Study of novel genes identified using forward genetics is challenging but exciting, mutations in such disease genes can yield insights into new pathways and biological functions. In this report, we described an alteration of protein stability caused by point mutations in PNKD; this cellular membrane protein is likely involved in a reaction catalyzing metabolism of an α-hydroxythioester, and ablation or mutation of PNKD leads to a decrease in GSH levels in the brain. Findings from biochemical studies and mouse models will provide insight into the normal function of PNKD and dysfunction when mutated. Understanding of PNKD pathophysiology may facilitate understanding of the etiology of other movement disorders and lead to novel targets for development of therapies for this and other episodic disorders.

MATERIALS AND METHODS

SLG hydrolysis and luciferase assays

The SLG hydrolysis assay was performed in a 96-well plate. The concentration of SLG (0–2000 nM) was monitored by absorption at 240 nm using the Spectra Max 190 (Molecular Devices). Kinetic measurement of SLG hydrolysis was detected by the changes in SLG concentration as a function of the reaction time in the presence of 200 μM 5,5′-dithiobis(2-niotrobenzoate). Reactions were carried out at 37°C in 200 μl Tris–HCl, pH 7.5 with a range of SLG (0–2000 nM) and ∼10 ng of purified protein. HAGH and human PNKD-L protein concentrations were measured with the BCA Protein Assay Kit (Pierce) and equal amounts of protein were assayed in each well. Data are from three

independent experiments and are analyzed by SigmaPlot 11.0. Renilla luciferase was used as an internal control of transfection efficiency in cell culture experiments. Luciferase activity was measured using a Dual Luciferase Assay Kit (Promega) on the Genios Pro (Tecan).

Generation of transgenic and knockout flies

Drosophila HAGH null animals ($dhagh^{EX10}$) were generated by excising a transposable element in *dhagh* (P[SUPor-P] $CG4365^{KG07968}$, Bloomington Stock #14677). This removed 837 bp from the HAGH coding region which was verified by northern blot analysis and sequencing (data not shown). Enzymatic tests of protein extracts from this viable fly strain revealed no remaining HAGH activity. Human *UAS-Pnkd-L* transgenics were made by placing the coding region of *Pnkd-L* into pUAST which was injected into embryos with a transposase plasmid to generate a stable genomic insertion of the transgene. *dhagh* was cloned by reverse transcription polymerase chain reaction (RT-PCR) and placed into pUAST to generate the *UAS-DHAGH* transgenic animal. These transgenes were expressed by driving with daughterless-GAL4 in a homozygous $dhagh^{EX10}$ background to test the ability of each transgene to rescue HAGH activity. All clones were sequence confirmed.

Drosophila HAGH enzymatic assay

Each sample was prepared by collecting five flies of the appropriate genotype. Flies were mechanically ground and sonicated in a 10 mM sodium phosphate buffer solution (pH 7.4). Samples were spun down in a table top centrifuge (10 min at 14 000 rpm in 4°C) and the supernatant was removed and spun a second time in an ultracentrifuge (30 min at 50 000*g*, 4°C). Protein concentrations from the second centrifugation were measured and 8 μg of protein/sample was loaded into a 96-well plate with 50 mM Tris–HCl buffer (pH 7.4) and 3 mM *S*-lactoylglutathione. SLG concentrations were measured at 240 nm at 1 min increments for 30 min using the Spectra Max 190 (Molecular Devices).

mut-Tg mice and Pnkd knockout mice

Mutant *Pnkd* transgene mice were made using a mouse BAC carrying A7V and A9V mutations in the mouse *Pnkd* ortholog; *Pnkd* null mice were made by deleting exons 5–9 of the mouse *Pnkd* ortholog. Generation and characterization of these two lines are described in a separate manuscript (Lee *et al.*, submitted for publication).

GSH assay in mut-Tg and Pnkd knockout mice

Three-month-old *mut-Tg*, *PnkdD* null mice and WT littermates were sacrificed and cerebral cortices were harvested, weighed, snap frozen in liquid nitrogen and stored at −80°C for later protein extraction and total glutathione assays. Total glutathione in mouse brain extracts was analyzed using a Total Glutathione Quantification Kit (Dojindo) on a Spectra Max 190 (Molecular Devices). Results were normalized according to brain sample weight.

Plasmids and antibodies

Full-length cDNAs of three human *PNKD* isoforms were previously described (4). PNKD disease mutations (A7V/A9V, A33P) were introduced into human *PNKD* constructs (L and S isoforms) with the QuikChange XL Site-Directed Mutagenesis Kit (Stratagene). Two additional mutations in the region of the PNKD mutations (A15G/R16G), and a mutation further away from the N-terminus (C85G) were also engineered into the *PNKD-L* and *PNKD-S* constructs. Subclones of *PNKD*-L were obtained by RT–PCR from human brain cDNA using Expanded High Fidelity PCR (Roche). HAGH was obtained by RT–PCR from human brain cDNA. Full-length or domains of genes of interest were constructed on pCMV-Tag2 (Stratagene), pEF6/Myc-His (Invitrogen), pEGFP-N1 and pEGFP-C3 (Clontech) vectors using appropriate restriction enzyme sites to generate fusion proteins. All constructs were sequence confirmed. Constructs in Figure 6B encoded the following PNKD-L amino acid residues: (i) 75–385, (ii) 93–385, (iii) 132–385 and (iv) 167–385.

A Rabbit antibody (C2235) was raised against the C-terminus peptide of PNKD (DDYSRAQLLEELRRLKDMHKSK, 363–385) (Lee *et al.*, submitted for publication). Anti-GFP (ab290) and anti-M6PR (ab12894) are from Abcam, anti-Flag (F7425) is from Sigma, anti-glyceraldehyde 3-phosphate dehydrogenase (GAPDH) (MAB374) is from Chemicon, chicken anti-HAGH (A21981) is from GenWay and anti-Flag M2-conjugated agarose is from Sigma.

Cell culture, transfection and immunofluorescence

SH-SY5Y cells were maintained in the 1:1 mixture of Eagle's minimum essential medium and Ham's F12 Medium supplemented with heat-inactivated fetal bovine serum, 10% (v/v). HEK293 (ATCC) cells were maintained in Dulbecco's modified Eagle's medium (DMEM) supplemented with 10% (v/v) heat-inactivated fetal bovine serum. For protein expression and luciferase assays, HEK293 cells were seeded in 60 mm dishes or 12-well plates overnight, and transfected with plasmid using Lipofectamine 2000 (Invitrogen) when they reached 80–90% confluence. Cells were harvested 24 h post-transfection. SH-SY5Y cells were cultured on two-well slides. Cells were fixed with 4% paraformaldehyde solution and subjected to a standard immunostaining protocol.

Co-immunoprecipitation and western blot

HEK293 cells were transfected with Tag2B-*PNKD-L* and N1-*PNKD-L* constructs. Cells were harvested 24 h post-transfection, lysed with M-PER (PIERCE) reagent supplemented with benzonase nuclease (Novagen) and complete protease inhibitors (Roche). Soluble lysate was incubated with M2 agarose (Sigma) overnight at 4°C. M2 agarose was washed five times with 0.25% Triton X-100 PBS followed by three times with 0.5% Triton X-100 PBS, then bound protein was eluted using 1X Sample Loading Buffer (Invitrogen) and heated to 100°C for 5 min. Lysate and eluate were resolved on 10% glyceraldehyde 3-phosphate dehydrogenase (SDS-PAGE) gels, transferred to NC membranes (Millipore)

and probed with antibody according to a standard western blotting protocol.

Pulse chase assay

HEK293 cells were transfected with plasmids expressing Tag2B-*PNKD-L WT* or Tag2B-*PNKD-L MUT*. After 24 h, transfected cells were washed twice with fresh culture medium and starved for 1 h in DMEM without L-methionine and L-cysteine (Gibco). Fresh culture medium containing ^{35}S labeled cysteine/methionine (EXPRE35S, PerkinElmer Life Sciences) at 200 μCi/ml was then added. After 20 min of incubation, the radioactive medium was removed and the cells were washed three times with fresh DMEM supplemented with 10% (v/v) heat-inactivated fetal bovine serum and incubated at 37°C. At each time point (0, 10, 20, 40 and 60 min), cells were washed twice with PBS, harvested and lysed in M-PER lysis buffer (PIERCE) supplemented with complete protease inhibitors (Roche). Flag-*PNKD-L* was immunoprecipitated with anti-flag M2 agarose (Sigma), resolved on SDS–PAGE gels and subjected to radiography.

Quantitative real-time PCR analysis

Total RNA was isolated from freshly harvested mouse cortex using RNeasy Midi Kit (Qiagen), and 2 μg total RNA from each sample was used for reverse transcription using cDNA reverse transcription kit according to the manufacturer's instructions (Invitrogen). Genomic DNA was removed by DNase digestion. Quantitative real-time PCR was performed using a 7900HT FAST Real-time PCR System with SYBR Green reagents (Applied Biosystems). Dilution series and standard curves of Pnkd and GAPDH were amplified on each plate for each experiment. Transcript levels for PNKD were normalized to GAPDH mRNA levels according to the standard procedures.

SUPPLEMENTARY MATERIAL

Supplementary material is available at *HMG* online.

ACKNOWLEDGEMENTS

The authors are grateful to Drs Sarah Calvo and Vamsi Mootha for help in mining the mitoCarta database, to Drs Chakrapani Kalyanaraman and Matt Jacobson for helpful discussions and to Dr Devon Ryan for critical reading of the manuscript.

Conflict of Interest statement. None declared.

FUNDING

This work was supported by a Fellowship from the Dystonia Medical Research Foundation (Y.S.), a Bachmann Strauss Dystonia and Parkinson Foundation grant (L.J.P.), the Sandler Neurogenetics fund (L.J.P.) and National Institutes of Health grant NS043533 (L.J.P.). L.J.P. is an Investigator of the Howard Hughes Medical Institute. Funding to pay the Open Access publication charges for this article was provided by the Howard Hughes Medical Institute.

REFERENCES

1. Müller, U., Steinberger, D. and Németh, A.H. (1998) Clinical and molecular genetics of primary dystonias. *Neurogenetics*, **1**, 165–177.
2. Aguiar, C.P.M. and Ozelius, L.J. (2002) Classification and genetics of dystonia. *Lancet Neurol.*, **1**, 316–325.
3. Németh, A.H. (2002) The genetics of primary dystonias and related disorders. *Brain*, **125**, 695–721.
4. Lee, H.Y., Xu, Y., Huang, Y., Ahn, A.H., Auburger, G.W., Pandolfo, M., Kwiecinski, H., Grimes, D.A., Lang, A.E., Nielsen, J.E. *et al.* (2004) The gene for paroxysmal non-kinesigenic dyskinesia encodes an enzyme in a stress response pathway. *Hum. Mol. Genet.*, **13**, 3161–3170.
5. Bruno, M.K., Lee, H.Y., Auburger, G.W., Friedman, A., Nielsen, J.E., Lang, A.E., Bertini, E., Van Bogaert, P., Averyanov, Y., Hallett, M. *et al.* (2007) Genotype-phenotype correlation of paroxysmal nonkinesigenic dyskinesia. *Neurology*, **68**, 1782–1789.
6. Ghezzi, D., Viscomi, C., Ferlini, A., Gualandi, F., Mereghetti, P., DeGrandis, D. and Zeviani, M. (2009) Paroxysmal non-kinesigenic dyskinesia is caused by mutations of the MR-1 mitochondrial targeting sequence. *Hum. Mol. Genet.*, **18**, 1058–1064.
7. Thornalley, P.J. (1993) The glyoxalase system in health and disease. *Mol. Aspects Med.*, **14**, 287–371.
8. Grillo, M.A. and Colombatto, S. (2008) Advanced glycation end-products (AGEs): involvement in aging and in neurodegenerative diseases. *Amino Acids*, **35**, 29–36.
9. John, D.H. and Lesley, I.M. (1999) Glutathione and glutathione-depenent-enzymes represent a co-ordinately regulated defense against oxidative stress. *Free Radic. Res.*, **31**, 273–300.
10. Ceccon, M., Giusti, P., Facci, L., Borin, G., Imbesi, M., Floreani, M. and Skaper, S.D. (2000) Intracellular glutathione levels determine cerebellar granule neuron sensitivity to excitotoxic injury by kainic acid. *Brain Res.*, **862**, 83–89.
11. Schulz, J.B., Lindenau, J., Seyfried, J. and Dichgans, J. (2000) Glutathione, oxidative stress and neurodegeneration. *Eur. J. Biochem.*, **267**, 4904–4911.
12. Nagao, M., Fujita, Y., Sugimura, T. and Kosuge, T. (1986) Methylglyoxal in beverages and foods: its mutagenicity and carcinogenicity. *IARC Sci. Publ.*, **70**, 283–291.
13. Cameron, A.D., Ridderstom, M., Olin, B. and Mannervik, B. (1999) Crystal structure of human glyoxalase II and its complex with a glutathione thiolester substrate analogue. *Structure*, **7**, 1067–1078.
14. Wendler, A., Irsch, T., Rabbani, N., Thornalley, P.J. and Krauth-Siegel, R.L. (2009) Glyoxalase II does not support methylglyoxal detoxification but serves as a general trypanothione thioesterase in African trypanosomes. *Mol. Biochem. Parasitol.*, **163**, 19–27.
15. Satoh, T., Ishige, K. and Sagara, Y. (2004) Protective effects on neuronal cells of mouse afforded by ebselen against oxidative stress at multiple steps. *Neurosci. Lett.*, **371**, 1–5.
16. Cadeta, J.L. and Brannocka, C. (1998) Free radicals and the pathobiology of brain dopamine systems. *Neurochem. Int.*, **32**, 117–131.
17. Chi, L., Ke, Y., Luo, C., Gozal, D. and Liu, R. (2007) Depletion of reduced glutathione enhances motor neuron degeneration *in vitro* and *in vivo*. *Neuroscience*, **144**, 991–1003.
18. Armstrong, J.S., Steinauer, K.K., Hornung, B., Irish, J.M., Lecane, P., Birrell, G.W., Peehl, D.M. and Knox, S.J. (2002) Role of glutathione depletion and reactive oxygen species generation in apoptotic signaling in a human B lymphoma cell line. *Cell Death Differ.*, **9**, 252–263.
19. Pereira, C.F. and Oliveira, C.R. (2000) Oxidative glutamate toxicity involves mitochondrial dysfunction and perturbation of intracellular Ca2+ homeostasis. *Neurosci. Res.*, **37**, 227–236.
20. Hou, J.G., Cohen, G. and Mytilineou, C. (1997) Basic fibroblast growth factor stimulation of glial cells protects dopamine neurons from 6-hydroxydopamine toxicity: involvement of the glutathione system. *J. Neurochem.*, **69**, 76–83.
21. Schuchmann, S. and Heinemann, U. (2000) Diminished glutathione levels cause spontaneous and mitochondria-mediated cell death in neurons from trisomy 16 mice: a model of Down's syndrome. *J. Neurochem.*, **74**, 1205–1214.

22. Gordon, K.L. and Gonzalez-Alegre, P. (2008) Consequences of the DYT1 mutation on torsinA oligomerization and degradation. *Neuroscience*, **157**, 588–595.
23. Giles, L.M., Chen, J., Li, L. and Chin, L.S. (2008) Dystonia-associated mutations cause premature degradation of torsinA protein and cell-type-specific mislocalization to the nuclear envelope. *Hum. Mol. Genet.*, **17**, 2712–2722.
24. Goodchild, R.E., Kim, C.E. and Dauer, W.T. (2005) Loss of the dystonia-associated protein torsinA selectively disrupts the neuronal nuclear envelope. *Neuron*, **48**, 923–932.
25. Torres, G.E., Sweeney, A.L., Beaulieu, J.M., Shashidharan, P. and Caron, M.G. (2004) Effect of torsinA on membrane proteins reveals a loss of function and a dominant-negative phenotype of the dystonia-associated DeltaE-torsinA mutant. *Proc. Natl Acad. Sci. USA*, **101**, 15650–15655.
26. Zhao, Y., DeCuypere, M. and LeDoux, M.S. (2008) Abnormal motor function and dopamine neurotransmission in DYT1 DeltaGAG transgenic mice. *Exp. Neurol.*, **210**, 719–730.
27. Hewett, J.W., Tannous, B., Niland, B.P., Nery, F.C., Zeng, J., Li, Y. and Breakefield, X.O. (2007) Mutant torsinA interferes with protein processing through the secretory pathway in DYT1 dystonia cells. *Proc. Natl Acad. Sci. USA*, **104**, 7271–7276.
28. Misbahuddin, A., Placzek, M.R., Taanman, J.W., Gschmeissner, S., Schiavo, G., Cooper, J.M. and Warner, T.T. (2005) Mutant torsinA, which causes early-onset primary torsion dystonia, is redistributed to membranous structures enriched in vesicular monoamine transporter in cultured human SH-SY5Y cells. *Mov. Disord.*, **20**, 432–440.
29. Wichmann, T. (2008) Commentary: dopaminergic dysfunction in DYT1 dystonia. *Exp. Neurol.*, **212**, 242–246.
30. Pagliarini, D.J., Calvo, S.E., Chang, B., Sheth, S.A., Vafai, S.B., Ong, S.E., Walford, G.A., Sugiana, C., Boneh, A., Chen, W.K. *et al.* (2008) A mitochondrial protein compendium elucidates complex I disease biology. *Cell*, **134**, 112–123.